AFRL-SR-BL-TR-99-

0147

REPORT DOCUMENTATION PAGE

1. AGENCY USE ONLY (Leave blank)	2. REPORT DATE	3. REPORT TYPE AND DATES COVERED
	5/31/99	Final Tech.: Dec. 1 1996 - Feb. 28 1999

4. TITLE AND SUBTITLE
Large eddy simulation of turbulent flow over an airfoil using unstructured grids

5. FUNDING NUMBERS
F49620-97-1-0043

6. AUTHOR(S)
Kenneth E. Jansen

7. PERFORMING ORGANIZATION NAME(S) AND ADDRESS(ES)
Rensselaer Polytechnic Institute
110 8th St
Troy, NY 12180

8. PERFORMING ORGANIZATION REPORT NUMBER
A10767

9. SPONSORING / MONITORING AGENCY NAME(S) AND ADDRESS(ES)
AFOSR/NA
801 N. Randolf St. Room 732
Arlington, VA 22203-1977

10. SPONSORING / MONITORING AGENCY REPORT NUMBER

19990614 014

11. SUPPLEMENTARY NOTES

12a. DISTRIBUTION / AVAILABILITY STATEMENT
Approved for public release; distribution is unlimited

12b. DISTRIBUTION CODE

13. ABSTRACT *(Maximum 200 Words)*
Many flows of aeronautical interest have regions where turbulence has a significant effect. For many of these flows, Reynolds-averaged Navier-Stokes simulation (RANSS) techniques do not give an acceptable description of the flow. In these cases a more detailed simulation of the turbulence is required. One such detailed simulation technique, large-eddy simulation (LES) has matured to the point of application to complex flows. Historically, LES have been carried out with structured grids which suffer from two major difficulties: the extension to higher Reynolds numbers leads to an impractical number of grid points, and most real world flows are rather difficult to represent geometrically with structured grids. Unstructured-grid methods offer a release from both of these constraints. Within this sponsored research significant progress has been made towards the application of the above approach to flows of aeronautical interest.

14. SUBJECT TERMS
Turbulence, Large eddy simulation, Unstructured grid CFD, Airfoil, Separated flow, Dynamic subgrid-scale model

15. NUMBER OF PAGES
16

16. PRICE CODE

17. SECURITY CLASSIFICATION OF REPORT	18. SECURITY CLASSIFICATION OF THIS PAGE	19. SECURITY CLASSIFICATION OF ABSTRACT	20. LIMITATION OF ABSTRACT
Unclassified	Unclassified	Unclassified	

A final report for

Large eddy simulation of turbulent flow over an airfoil using unstructured grids

Submitted by

Kenneth E. Jansen

Department of Mechanical Engineering,
Aeronautical Engineering and Mechanics
110 8th St.
Troy, NY 12180-3590
Phone 518-276-6755

Submitted to

Dr. Leonidas Sakell

Air Force Office of Scientific Research
Ballston Tower 2
Rosylyn, VA
Phone 703 696-6566

For the period of

December 1, 1996–February 28, 1999

Abstract

Many flows of aeronautical interest have regions where turbulence has a significant effect. For many of these flows, Reynolds-averaged Navier-Stokes simulation (RANSS) techniques do not give an acceptable description of the flow. In these cases a more detailed simulation of the turbulence is required. One such detailed simulation technique, large-eddy simulation (LES) has matured to the point of application to complex flows. Historically, LES have been carried out with structured grids which suffer from two major difficulties: the extension to higher Reynolds numbers leads to an impractical number of grid points, and most real world flows are rather difficult to represent geometrically with structured grids. Unstructured-grid methods offer a release from both of these constraints. Within this sponsored research significant progress has been made towards the application of the above approach to flows of aeronautical interest.

1 Introduction

Computation of turbulence can be carried out in three distinct ways: direct numerical simulation (DNS), where the computational method resolves all of the turbulent motions (from the largest scale down to the scale where motion is converted to heat via viscous dissipation), LES, where the large eddies carrying most of the energy are resolved by the computational method (leaving the small or subgrid-scale (SGS) eddies to be modeled), and RANSS, where no attempt is made to resolve any of the turbulent motions (rather, the net effect of these motions upon the mean flow is modeled). DNS can be expected to remain out of reach of most engineering problems for several years. RANSS, though computationally efficient for some steady flows, has been disappointing for unsteady and/or complex flows. Therefore, LES, has been identified as the most promising turbulence simulation tool for the near future.

Over the past three decades, a significant amount of research has been devoted to LES. The overwhelming majority of this research has been carried out with spectral or structured grid finite difference methods. While much has been learned about the basic physics of turbulence using these approaches, they suffer from two significant problems: difficulty in application to arbitrarily complex geometries, and a rapid increase in the number of degrees of freedom necessary to describe flows at typical engineering Reynolds numbers. Recently, LES has been extended to finite element methods on unstructured grids ([1],[2]) with near perfect parallel scaling on a variety of different computing platforms [3]. This extension not only facilitates simulation of flows within or around complex geometries found in engineering applications, but also allows great reductions in computational effort through the ability of unstructured grids to adapt locally to fine scale structures in one flow region while remaining coarse in regions where the structures are large. Already, these methods have realized a 27 fold point reduction over an equivalent-resolution structured grid (i.e. to make a structured grid which matches the resolution in the finest regions of the unstructured grid would require a factor of 27 times as many points assuming the stretched mesh can be mapped to a cube ([4],[5])).

2 Method and advances under AFOSR support

2.1 Finite element formulation

There are many finite element and finite volume formulations available for application with unstructured grids. However, few have had their accuracy and stability as carefully scrutinized as what have become known as stabilized finite element methods. Two important members of this family, Galerkin/Least-Squares (GLS) and Streamline Upwind Petrov Galerkin (SUPG), have been proven stable and higher order accurate (converging at the optimal rate for a given function space) for flows ranging from inviscid to viscous dominated. The early analyses were done in the context of multi-dimensional linear advective-diffusive systems (see Hughes *et al.* [6] and Hughes *et al.* [7]) and later followed by an analysis of the frozen coefficient Navier-Stokes equations (see Franca and Hughes [8]). The interested reader is encouraged to look to these references for detail as the space of this report allows only a summary of the formulation.

Consider the compressible Navier-Stokes equations (complete with continuity and total energy equations) written in filtered form after the application of a subgrid-scale model (see Moin

et al. [9], Moin & Jimenéz [10], Germano *et al.* [11] or section 2.3).

$$\boldsymbol{U}_{,t} + \boldsymbol{F}^{\text{adv}}_{i,i} - \boldsymbol{F}^{\text{diff}}_{i,i} = \boldsymbol{\mathcal{S}} \tag{1}$$

where

$$\boldsymbol{U} = \left\{ \begin{array}{c} U_1 \\ U_2 \\ U_3 \\ U_4 \\ U_5 \end{array} \right\} = \overline{\rho} \left\{ \begin{array}{c} 1 \\ \tilde{u}_1 \\ \tilde{u}_2 \\ \tilde{u}_3 \\ \tilde{e}_{\text{tot}} \end{array} \right\}, \qquad \boldsymbol{F}^{\text{adv}}_i = \tilde{u}_i \boldsymbol{U} + \overline{p} \left\{ \begin{array}{c} 0 \\ \delta_{1i} \\ \delta_{2i} \\ \delta_{3i} \\ \tilde{u}_i \end{array} \right\}, \qquad \boldsymbol{F}^{\text{diff}}_i = \left\{ \begin{array}{c} 0 \\ \tau_{1i} \\ \tau_{2i} \\ \tau_{3i} \\ \tau_{ij}\tilde{u}_j - q_i \end{array} \right\} \tag{2}$$

and

$$\tau_{ij} = 2(\mu + \mu_T)(S_{ij}(\tilde{\boldsymbol{u}}) - \frac{1}{3} S_{kk}(\tilde{\boldsymbol{u}})\delta_{ij}) \quad , \quad S_{ij}(\tilde{\boldsymbol{u}}) = \frac{\tilde{u}_{i,j} + \tilde{u}_{j,i}}{2} \tag{3}$$

$$q_i = -(\kappa + \kappa_T)\tilde{T}_{,i} \quad , \quad \kappa_T = c_p \frac{\mu_T}{Pr_T} \quad , \quad \tilde{e}_{\text{tot}} = \tilde{e} + \frac{\tilde{u}_i \tilde{u}_i}{2} \quad , \quad \tilde{e} = c_v \tilde{T} \tag{4}$$

Here, we use the overbar to denote an unweighted filter and a tilde to denote a density weighted filter. The filtered variables are: the velocity $\tilde{u}_i$, the pressure $\overline{p}$, the density $\overline{\rho}$, the temperature $\tilde{T}$ and the total energy $\tilde{e}_{\text{tot}}$. The constitutive laws relate the stress, τ_{ij}, to the deviatoric portion of the strain, $S^d_{ij} = S_{ij} - \frac{1}{3}S_{kk}\delta_{ij}$, through a molecular viscosity, μ, plus turbulent viscosity, μ_T. Similarly, the heat flux, q_i, is proportional to the gradient of temperature with the proportionality constant given by the addition of a molecular conductivity, κ, and a turbulent conductivity, κ_T, which is assumed proportional to the turbulent viscosity as described above. While the formulation is not limited to an ideal gas, $\overline{p} = \overline{\rho} R \tilde{T}$, and constant specific heats at constant pressure, c_p, and at constant volume, c_v, that is the model used in the calculations shown in this report. Furthermore, since all the calculations shown in this report are at low Mach number where temperature variation is low we have also assumed a constant molecular viscosity and constant conductivity through a constant Prandtl number, though, this again is not a necessary simplification. Finally $\boldsymbol{\mathcal{S}}$ is a body force (or source) term.

For the specification of the methods that follow, it is helpful to define the quasi-linear operator (with respect to some yet to be determined variable vector $\boldsymbol{Y}$) related to (1) as

$$\boldsymbol{\mathcal{L}} \equiv \boldsymbol{A}_0 \frac{\partial}{\partial t} + \boldsymbol{A}_i \frac{\partial}{\partial x_i} - \frac{\partial}{\partial x_i}(\boldsymbol{K}_{ij} \frac{\partial}{\partial x_j}) \tag{5}$$

from which $\boldsymbol{\mathcal{L}}$ can be naturally decomposed into time, advective, and diffusive portions

$$\boldsymbol{\mathcal{L}} = \boldsymbol{\mathcal{L}}_{\text{t}} + \boldsymbol{\mathcal{L}}_{\text{adv}} + \boldsymbol{\mathcal{L}}_{\text{diff}}. \tag{6}$$

Here $\boldsymbol{A}_i = \boldsymbol{F}^{\text{adv}}_{i,\boldsymbol{Y}}$ is the i^{th} Euler Jacobian matrix, $\boldsymbol{K}_{ij}$ is the diffusivity matrix, defined such that $\boldsymbol{K}_{ij}\boldsymbol{Y}_{,j} = \boldsymbol{F}^{\text{diff}}_i$, and $\boldsymbol{A}_0 = \boldsymbol{U}_{,\boldsymbol{Y}}$ is the change of variables metric. For a complete description of $\boldsymbol{A}_0$,$\boldsymbol{A}_i$ and $\boldsymbol{K}_{ij}$, the reader is referred to [12]. Using this, we can write (1) as simply $\boldsymbol{\mathcal{L}Y} = \boldsymbol{\mathcal{S}}$.

To proceed with the finite element discretization of the Navier-Stokes equations (1), we must define some notation. First, let $\bar{\Omega}$ represent the closure of the physical spatial domain (i.e. $\Omega \cup \Gamma$ where Γ is the boundary). Next, Ω, is discretized into n_{el} finite elements, Ω^e. To derive the weak form of (1), the entire equation is dotted from the left by a vector of weight functions,

$\boldsymbol{W}$, and integrated over the spatial domain. Integration by parts is then performed to move the spatial derivatives onto the weight functions (reducing the continuity requirements). This process leads to the integral equation (often referred to as the weak form): find $\boldsymbol{Y}$ such that

$$\begin{aligned} 0 &= \int_\Omega \left(\boldsymbol{W} \cdot \boldsymbol{U}_{,t} - \boldsymbol{W}_{,i} \cdot \boldsymbol{F}_i^{\text{adv}} + \boldsymbol{W}_{,i} \cdot \boldsymbol{F}_i^{\text{diff}} \right) d\Omega - \int_\Gamma \boldsymbol{W} \cdot \left(-\boldsymbol{F}_i^{\text{adv}} + \boldsymbol{F}_i^{\text{diff}} \right) n_i \, d\Gamma \\ &+ \sum_{e=1}^{n_{el}} \int_{\Omega^e} \boldsymbol{\mathcal{L}}^T \boldsymbol{W} \cdot \boldsymbol{\tau} \left(\boldsymbol{\mathcal{L}} \boldsymbol{Y} - \boldsymbol{\mathcal{S}} \right) d\Omega \end{aligned} \tag{7}$$

The first line of (7) contains the Galerkin approximation (interior and boundary) and the second line contains the least-squares stabilization. SUPG stabilization is obtained by replacing $\boldsymbol{\mathcal{L}}^T$ by $\boldsymbol{\mathcal{L}}_{\text{adv}}^T$. The stabilization matrix $\boldsymbol{\tau}$ is an important ingredient in these methods and is well documented in Shakib [13] and in Franca and Frey [14]. Note that we have chosen to find $\boldsymbol{Y}$ instead of $\boldsymbol{U}$. As discussed in Hauke and Hughes [15], $\boldsymbol{U}$ is often not the best choice of solution variables, particularly when the flow is nearly incompressible. For the calculations performed herein, the SUPG stabilized method was applied with linearly interpolated pressure-primitive variables viz.

$$\boldsymbol{Y} = \left\{ \begin{array}{c} Y_1 \\ Y_2 \\ Y_3 \\ Y_4 \\ Y_5 \end{array} \right\} = \left\{ \begin{array}{c} \overline{p} \\ \tilde{u}_1 \\ \tilde{u}_2 \\ \tilde{u}_3 \\ \tilde{T} \end{array} \right\} \tag{8}$$

By inspecting (2)-(4) it is clear that all quantities appearing in (7) may be easily calculated from (8).

To develop a numerical method, the weight functions ($\boldsymbol{W}$), the solution variable ($\boldsymbol{Y}$), and its time derivative ($\boldsymbol{Y}_{,t}$) are expanded in terms of basis functions (typically piecewise polynomials; all calculations described herein were performed with linear basis). The integrals (7) are then evaluated using Gauss quadrature resulting in a system of non-linear ordinary differential equations which can be written as

$$\boldsymbol{M} \check{\boldsymbol{Y}}_{,t} = \boldsymbol{R}(\check{\boldsymbol{Y}}) \tag{9}$$

where the check is added to make clear that $\check{\boldsymbol{Y}}$ is the vector of solution values at discrete points (interpolated through the space by the basis functions) and $\check{\boldsymbol{Y}}_{,t}$ are the time derivative values at the same points. An implicit, second order accurate family of time integrators has been developed [16] for application to this problem. This new time integrator is an extension of Chung and Hulbert's generalized alpha method [17] to our first order system. The family is characterized by one free parameter, the amplification factor as the time step over the period of the frequency of interest tends to infinity, ρ_∞, which may be chosen to have a value between 0 (Gears Method) and 1 (Midpoint Rule). Full documentation of Chung and Hulbert's method extended to the Navier-Stokes equations is not possible in the confines of this report

but should appear in the literature shortly [16]. The method results in a non-linear matrix problem that is solved in a predictor-corrector format yielding successive linear problems. Each linear problem is solved using the Matrix-Free Generalized Minimal RESidual (MF-GMRES) solution technique with a block diagonal preconditioner developed by Johan *et al.* [18]. Convergence of the non-linear problem is confirmed before moving to the next time step. We have observed that there is little difference in the turbulent statistics between solving the equations

with two iterations (2.5-3.0 order of magnitude reduction) and three iterations (3.0-4.0 orders of magnitude reduction). There is of course a difference in the instantaneous signal after a long time integration as will always be the case when dealing with turbulence. It is interesting to note that even roundoff errors will eventually lead to a divergence of an instantaneous signal regardless of the level of solution. This is initially alarming until we remember that it is the turbulence statistics that we are most interested in predicting.

2.2 Parallel implementations

The original implementation of this approach was on a Thinking Machines CM5 following the so-called data parallel approach. Finite element methods are amenable to this approach since the bulk of the computational effort lies in evaluating local integrals over each element domain. Parallelization of these operations is trivial after a gather of the data from the global nodes to an element based data structure. After the element integrations are performed in parallel, the results (residuals of (9)) are then scattered (assembled) back to the nodes where the equations are solved.

On the CM5 these gather/scatter operations are performed using CMSSL library procedures requiring no pre-processing of the data. This made application to this platform quite easy. Unfortunately, other parallel platforms do not have libraries of this type. For this reason a second version of the code was developed, employing the Message Passing Interface (MPI) library to do the gather and scatter operations. This version of the code requires that the problem be pre-processed to break the computational domain into n pieces where n is the number of processors, on which, the problem will be run. This pre-processing step is non-trivial for unstructured grids since load balance (equal distribution of the elements onto each processor) and minimal communication are necessary. Recently we have accomplished this pre-processing procedure and have begun testing our MPI version of the code on a variety of platforms (IBM-SP2, SGI-Origin, SUN-Sparc and Cray J90). The algorithm has shown perfect scalability (see Bastin [19]) on moderate sized problems (typically the bigger the better) due to the low ratio of communication to calculation that is inherent in finite element methods. The MPI version of the code also performs the communication much more efficiently than the CMSSL version of the code. On the CM5, communication required 20-25% of the total CPU time. With the MPI code this percentage is reduced to 3-5%. While this improvement is dramatic, both methods still use the majority of the CPU time computing, making communication improvement have little impact. Greater efficiency gains require a reduction in the computational effort, even if it comes at some loss in communication efficiency.

2.3 Dynamic model development

The full development of the dynamic model requires more space than is available here. We refer the interested reader to [9], Moin & Jimenéz [10], Germano *et al.* [11]. Here we only summarize our implementation and improvements

Most LES models rest on the assumption that the subgrid-scale stresses can be modeled by

$$t_{ij}^d = -2\mu_T S_{ij}^d(\tilde{\boldsymbol{u}}) \tag{10}$$

where the eddy viscosity, μ_T, is usually given by the Smagorinsky model [20],

$$\mu_T = C\overline{\Delta}^2\overline{\rho}|S|, \qquad |S| = \sqrt{2S_{ij}S_{ij}} \tag{11}$$

where C is the so-called Smagorinsky "constant".

This "constant" proved very elusive to the researchers of the seventies and the eighties. After several studies it seemed clear that this "constant" in fact varied from flow to flow and, worse yet, seemed to be a function of position within even the simplest flows (especially in near wall regions). In the early nineties a dynamic procedure for determining the subgrid-scale viscosity was developed by Germano *et al.* [11]. In this procedure the value of the constant C is determined dynamically by comparing the solution and various functions of the solution obtained from the simulation to the same quantities passed through a filter

Applications of the Smagorinsky-based dynamic model flourished within the spectral methods community and the finite difference community where it gained wide acceptance. Use of this model on unstructured grids required an extension of the filtering operator. A variety of filtering operators were developed in [1]. Through our recent research ([5], [3], [2]), we have determined that the generalized top-hat filter represents the best balance between accuracy and efficiency.

2.4 Numerical simulations and validations

Reference publications [16, 21, 22, 23, 2, 24, 3, 25, 1, 26, 4, 5, 27] provide a full description of our work in this area but here we will summarize it as:

1. With the dynamic model disabled we used our code to predict the growth of the most unstable eigenmode of the Orr-Sommerfield equations [3]. In that reference we showed that our method is significantly more accurate than staggered-grid central differences, the workhorse of the LES community. Then, with the model turned back on we confirmed that the value of C vanished when the disturbance was adequately represented.

2. The dynamic model was validated by studying the decay of isotropic turbulence, where good prediction both of the decay rate and the shape of the spectra were observed [3].

3. The classic case of turbulent flow in a channel at $Re_\tau = 180$ was studied and compared to staggered-grid central difference results [3]. Again, superior accuracy was demonstrated.

4. Moving to more complex geometry, a turbulent flow over a cavity is currently being simulated ($Re_\theta = 3500, Re_H = 27000, M = 0.1$). Results have not been published but an instantaneous visualization of the streamwise vorticity is included here.

5. The airfoil simulation has been computed and is described in several references ([1],[4], [5],[3]). An instantaneous visualization of the isosurfaces of the spanwise velocity is included in Figure 2. The most challenging aspect of this flow is the prediction of smooth separation on the last 20% of the upper surface. The early LES predictions showed a larger separation than the RANSS simulations but still less than that of the experiments ([28],[29],[30]). Some insight into the reason for the disagreement can be obtained from Figure 3. Here, the calculation is in good agreement with the experimental data when

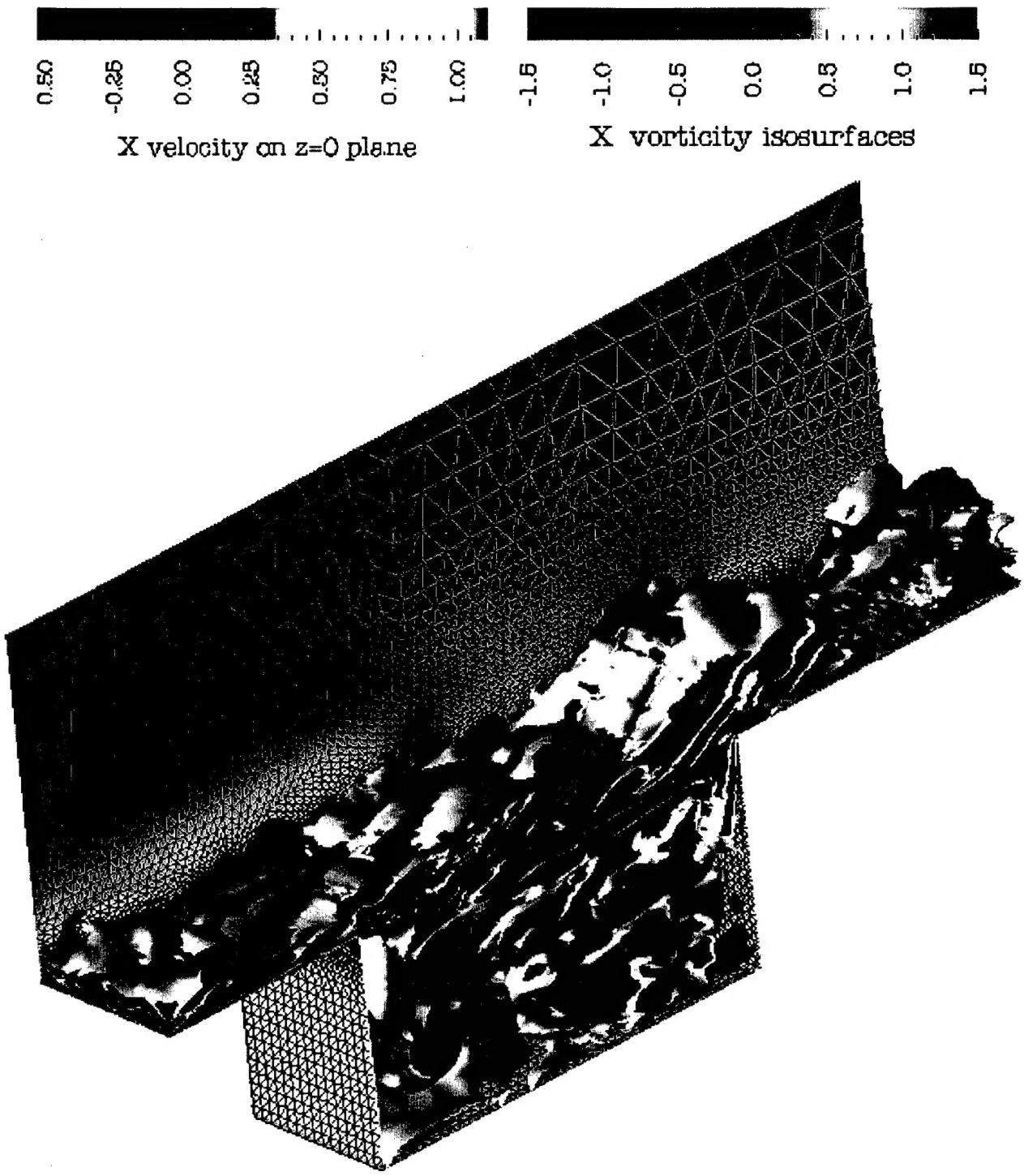

Figure 1: Isosurfaces of vorticity in a turbulent boundary layer flowing over a cavity.

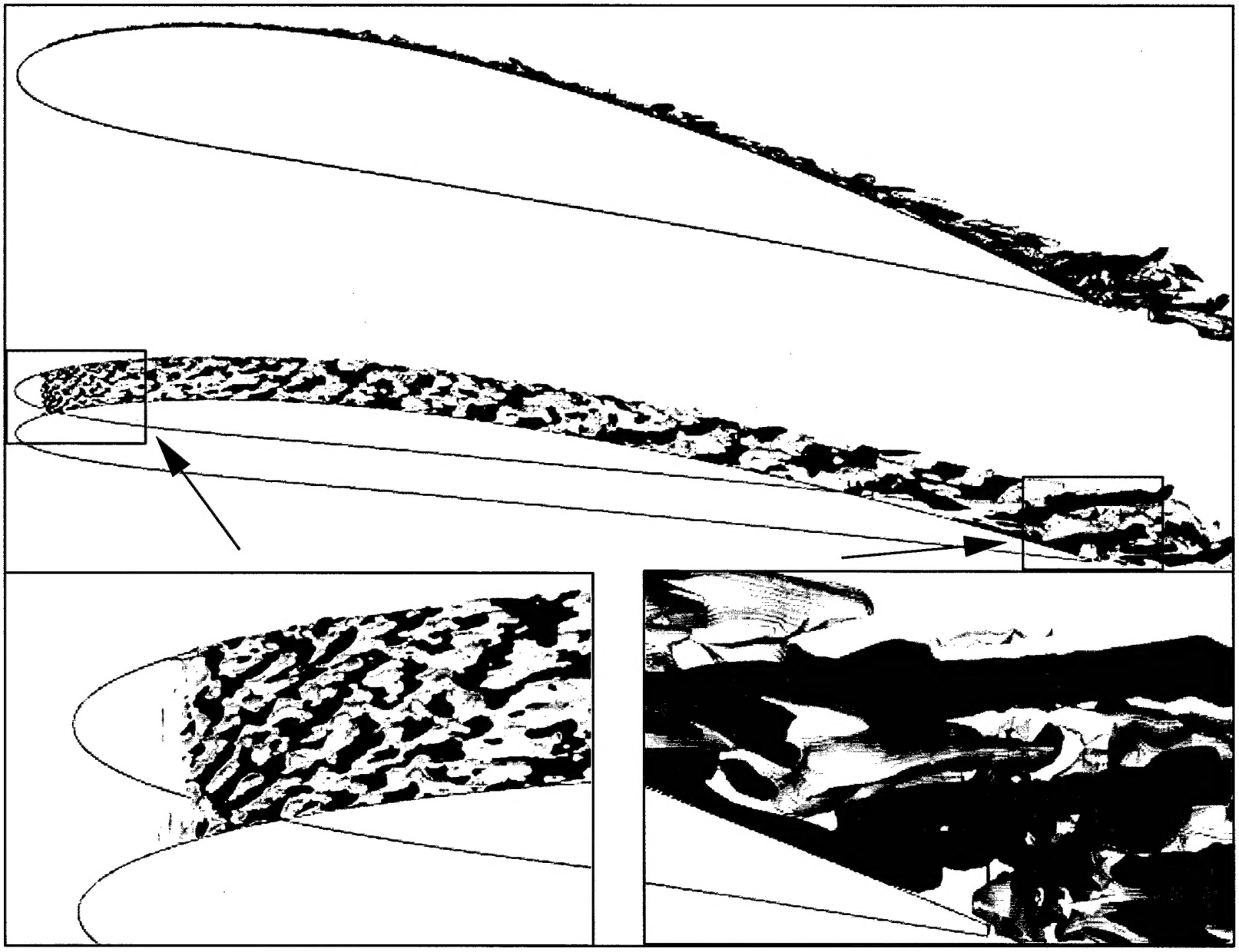

Figure 2: Tip-to-tail development of the turbulent structures identified by spanwise velocity isosurfaces in the boundary layer over the upper surface of the airfoil. Top figure provides a side view which illustrates the development of the boundary layer thickness. The middle figure tilts slightly to show the spanwise structures. Lower left figure zooms in on the early boundary layer while the lower right zooms on the tail region illustrating the dramatic variation in spatial scales.

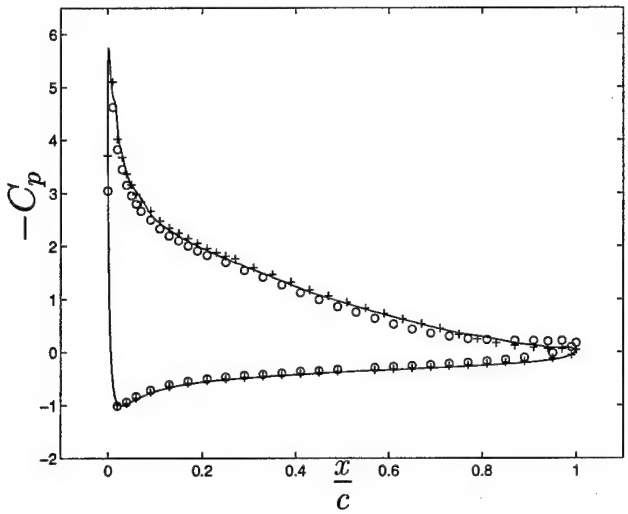

Figure 3: Coefficient of pressure on the airfoil surface comparing calculation (——) to Hasting's experiment with transition strip (o) and without transition strip (+).

there is no transition strip. However, there is a substantial flattening of the experimental C_p distribution in the trailing edge region when the transition strip was in place. This minor change in the C_p distribution signals a much more dramatic change in the velocity field where a much more massive separation would be expected. While it is encouraging that our calculation (which at this point had no transition strip) agrees with the experiment with the same boundary conditions, all velocity and stress data was taken with the transition strip in place. Therefore, in subsequent calculations we modified our boundary conditions to accurately represent both the wind tunnel walls and the serrated transition strip of Wadcock [30] as seen if Figure 4. Addition of these features did improve the agreement, but discrepancies remained. We believe that the remaining discrepancies are linked to the inadequate spanwise extent of our computational domain. Figure 5 shows the effect of doubling the spanwise domain width on the velocity profiles in the separated region. The obvious solution of further doubling the spanwise domain width is unattractive since it would again double the cost of the calculation. Instead, under other support, we are developing new boundary conditions to address this difficulty in a more cost effective manner.

6. The above computations were completed using only linear interpolation functions. We have recently implemented a new set of interpolation functions which utilize a hierarchical basis [21, 22]. With one input parameter change, we can change the order of accuracy of our method. We have confirmed that we obtain the theoretically optimal rate of convergence ($O(h^{p+1})$ in the L_2 norm where p is the polynomial order) for laminar channel flow and acoustic wave propagation and for Kovasnay flow. This approach adds p adaptivity to our already demonstrated capability in h adaptivity. While other researchers are also exploring this approach we should emphasize that we have successfully integrated this approach into our massively parallel, dynamic subgrid-scale model LES code. Therefore, we have removed all of the obstacles to large scale simulations with this approach. Indeed, turbulent simulations are underway at the time of this writing and preliminary results

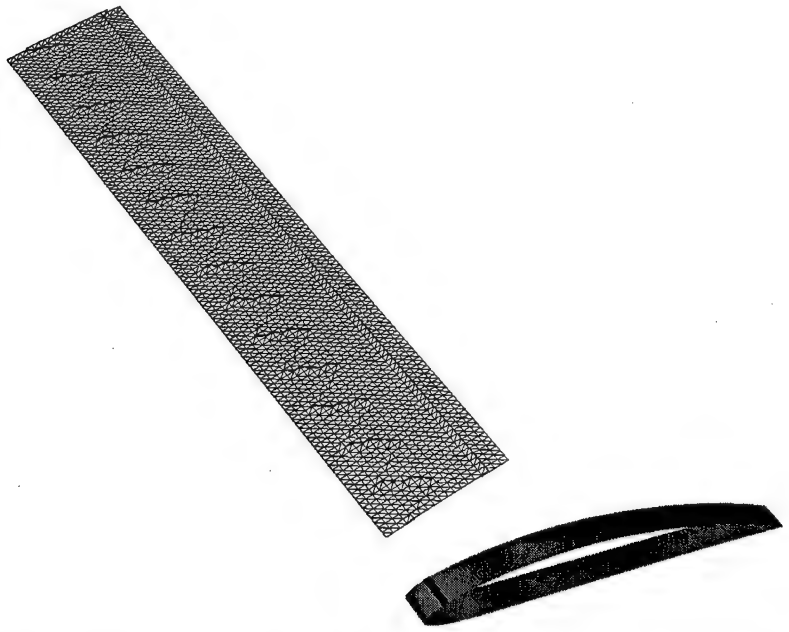

Figure 4: Geometric model of the exact shape, height and position (shown in black on the airfoil surface) of Wadcock's transition strip.

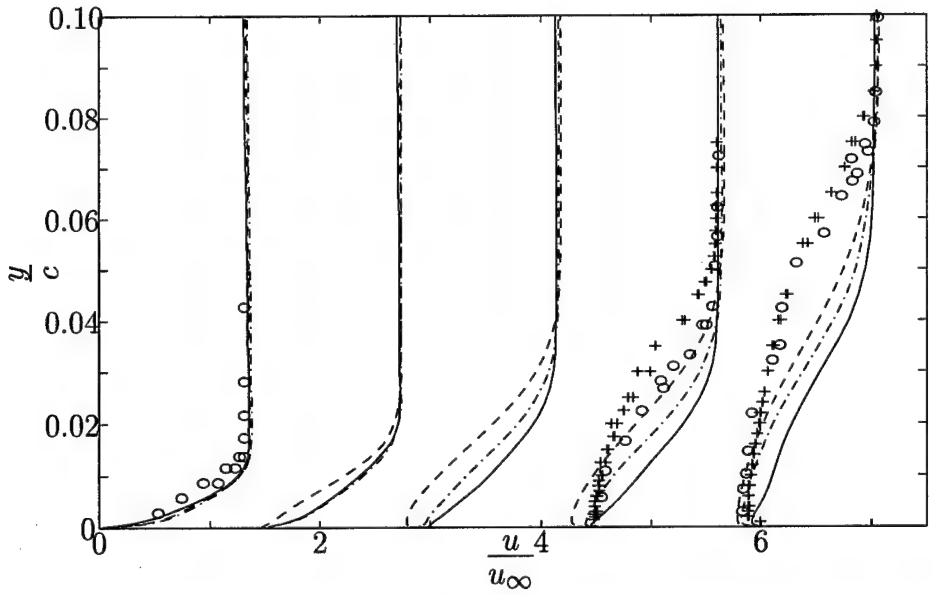

Figure 5: Profiles of tangential velocity component at various positions along the airfoil surface ($x/c = 0.59, 0.066, 0.78, 0.82, 0.95$, plots have been shifted by 1.5 at each station). Solutions correspond to: without wind tunnel walls or transition strip ——— , with wind tunnel walls and transition strip ($W/c = 0.025$) ---- , with wind tunnel walls and transition strip ($W/c = 0.05$) —·— , Wadcock ∘ , Hastings and Williams + .

are quite promising. We expect to present them at the Second AFOSR International Conference on DNS/LES.

2.4.1 Improved solver efficiency

We currently use a matrix-free generalized minimal residual method (MF-GMRES), which requires very low storage but is somewhat computationally intensive. Since memory is becoming more available on parallel machines we have investigated a new solver which takes advantage of the sparseness of our matrix, thereby enabling us to form the matrix which greatly reduces the computational effort at a minor cost to memory. Our current experience with the 8.5 million element airfoil simulation [2] suggests that this tradeoff will be a highly favorable one. Forming the matrix has a second benefit since it allows a much richer set of pre-conditioners to be employed (currently in the matrix-free technique, only block-diagonal pre-conditioning is possible), further accelerating convergence at each step. AFOSR support produced a Masters thesis on this topic which is in the process of being converted into a journal article (thesis is available by request).

2.4.2 New boundary conditions

A very promising avenue to improved simulations is through the introduction of new boundary conditions. Here we added two new types of boundary conditions to our method. The first, a sub-layer model, is somewhat classical. The second, and perhaps more novel, can best be described as a surface extraction boundary condition (SEBC). In the following paragraphs we describe each of these.

Wall layer modeling has been carried out since the early days of LES [31]. It is known to be a fairly good approximation for flows that are near equilibrium but can give disappointing results in other cases. The advent of unstructured-grid LES affords the opportunity to develop new wall layer models which, through their dependence on grid density could smoothly fair between a resolved-wall LES and a wall-layer-modeled LES. In this way, a full LES could be carried out in regions where it is necessary (i.e. where the flow is not in equilibrium and high accuracy is needed) and a wall layer model could be used elsewhere (where the flow is in equilibrium and/or accuracy requirements are lower). Existing wall layer models do not have this character and therefore new models must be developed. Again, we emphasize that the unstructured-grid LES approach offers: 1) the opportunity to resolve more interesting cases in the validation of these models, and 2) the capability to smoothly change the mesh spacing between the fine near wall spacing required in a resolved-wall LES and the coarse near wall resolution required for a wall-layer-modeled LES. We have completed preliminary testing of the wall layer model wherein we have applied it to channel and flat plate flows. Application to the airfoil is the next step.

Experience with the airfoil LES has identified a new boundary condition that will dramatically reduce the computational effort required in LES of problems with a solid surface whose dimension transverse to the mean flow direction is large (e.g. the leading edge of a wing). In problems of this type, what makes LES so expensive is the need to carry the fine resolution to resolve the turbulent fluctuations over a long transverse or spanwise dimension. To accurately model the turbulent fluctuations in this region only requires a very short spanwise dimension since they are known to have a fairly short two point correlation decay length (typically 600-800

wall units of spanwise extent are necessary to insure a de-correlated signal). That is to say, in the leading edge region, the same solution statistics would be obtained for a spanwise domain of 700 wall units, 7000 wall units, or even 70,000 wall units. Indeed this is the very principle upon which the spanwise periodic boundary condition is based. Typically we choose our spanwise domain length to be greater than the two point correlation decay length at all points.

In the airfoil simulation the two point correlation length changes by over an order of magnitude due to the strong adverse pressure gradient which drives the flow to separate in the last 20% of the chord length. Therefore, our current simulation is about 8 times wider than is necessary for the early turbulent boundary layer and perhaps is still too narrow in the trailing edge region. Indeed, when we compare the statistics of this solution to the statistics of the solution obtained on a grid with the exact same grid spacing but with half the spanwise length (translating into a factor of two savings in grid points), the early boundary layer is unchanged while the trailing edge boundary layer is adversely impacted. By examining Figure 2 one can see that the solution near the nose looks to be de-correlated in about one eighth of the domain (i.e. the typical eddy structure is about one sixteenth of the spanwise length), while the trailing edge boundary layer contains only one or two pairs of structures.

We have completed preliminary testing of a new boundary condition to alleviate this difficulty. This boundary condition allows the domain width to be doubled as necessary to maintain an adequate two point correlation decay length while maintaining computational efficiency. To correctly implement this boundary condition requires that we find the appropriate solution to apply as a boundary condition on the newly doubled surface. The appropriate solution is the solution from the plane that was just copied. The procedure is illustrated for the surface nodes in Figure 6. The process must be carried out for the plane extending from these nodes to the opposing boundary but for clarity we only show the line here. We name this boundary condition a surface extraction boundary condition (SEBC). The SEBC is effectively an inflow boundary condition where the solution value is set to that of a companion node on the interior plane. The process can be repeated as many times as is necessary with the only limitation being that the spanwise width must grow by an integer multiple of the previous spanwise width.

Though conceptually simple, there remain a number of challenges to realizing the efficiency gains of the SEBC. The key points that must be addressed in this research are:

1. An initial mesh is generated that is wide enough for the most narrow section,

2. The appropriate points to expand the domain are identified and the mesh is copied to create a discretely varying spanwise width (all of the nodes and elements between the red plane and the opposite boundary in Figure 6),

3. At the same time, the newly created nodes which fall on the inflow boundary are given a boundary condition which links them to the nodes that they were copied from (the nodes along the plane created by extending the purple line to the opposite boundary are linked to the nodes between the green line and the opposite boundary),

4. The other newly created nodes which fall on the other boundaries are given the appropriate boundary conditions, (including the periodic boundary condition which is transferred from the points which are now interior to the newly expanded cross sectional plane),

Figure 6: The surface extraction boundary condition is outlined. Beyond a certain x position the original narrow spanwise domain is doubled (shown in red). The inflow to the new domain (the plane between the purple line and the farfield boundary) is linked a plane on the interior of the original domain (the plane between the green line and the farfield boundary). The process is repeated again at a later section through a second doubling of the spanwise domain. We only show the surfaces here for clarity but we emphasize that the boundary condition applies to the newly created inflow planes.

5. Though this boundary condition does not initialize any energy into the new low wavenumber modes that are supported on the expanded domain, this is a spatially developing flow and these modes can be expected to grow in the new domain where they are no longer constrained by the periodic boundary condition. Preliminary testing on flate plate and channel flows has been completed with encouraging results. Application to more complex geomtries is underway.

As noted in [32], it is the boundary layer near the leading edge which has the most strict resolution requirements leading to the prohibitively large number of grid points required for wing geometries. This approach is expected to reduce the current airfoil simulation cost by an order of magnitude. The wing simulation cost is expected to drop by two to three orders of magnitude. These gains are possible because the leading edge region is the most likely region to satisfy the conditions mentioned above for application to spanwise inhomogeneous flows.

2.5 Project summary

The work summarized herein aggressively pushed the envelope of turbulence simulation through the development of more efficient methods, solvers, models, and boundary conditions.

3 Acknowledgments

It should be graciously acknowledged that we were the beneficiaries of a Defense University Research Initiative Program (DURIP) (F49620-97-1-0250 together with Mark Shephard and Joseph Flaherty) associated with our past AFOSR research, from which we obtained the 8 processor SGI Onyx2 described below. Furthermore, we have enjoyed considerable access to the massively parallel DOD computers which have strongly enabled our research thus far.

We have also greatly benefited from the SCOREC computational facilities include parallel processors, high-performance visualization facilities and a workstation environment. Parallel processing facilities include SCOREC parallel computers and extensive access to Rensselaer's IBM SP2 with 34 thin nodes and 2 fat nodes. SCOREC also has a SGI Onyx2 Computer system with 8 R10000 processors and 3.5 GBytes of memory which is critical for pre- and post-processing the enormous data sets associated with this level of simulation. Distributed parallel processing is performed using SMP machines consisting of 2 IBM G30 SMP units with 4 processors, and 3 2-processor Sun UltraSparcs. SCOREC's network is supported by two Bay Networks Centillion switches. The various SMP workstations will use ATM to provide high performance communication for parallel processing between these machines. High performance visualization is supported by an Infinite Reality Engine with 1 Raster Manager on the 8-processor Onyx2, 2 SGI Indigo2 Maximum Impacts with R10000, 3 SGI Indigo2 Extremes and 2 1-processor Sun UltraSparcs. The five Sun Ultras have Creator 3-D graphics. The system is served by a Sun Enterprise 450 file server and has a total of 100 GB of high speed disk storage. Additional workstations include 13 Sparc10's, 12 other Sun workstations, and 5 IBM workstations.

We also graciously acknowledge the support of an additional graduate student under the Augmentation Awards for Science and Engineering Research Training (AASERT) Program (F49620-97-1-0478), which was affiliated with the current AFOSR contract and continues

through June of 2000. The ambitious work described herein would not have been possible without this additional student support.

References

[1] K. E. Jansen, "Unstructured grid large eddy simulation of flow over an airfoil", in *Annual Research Briefs*, Center for Turbulence Research, NASA Ames / Stanford University, (1994) 161–173.

[2] K. E. Jansen, "A stabilized finite element method for computing turbulence", *Comp. Meth. Appl. Mech. Engng.*, (accepted for publication).

[3] K.E. Jansen, "Large-eddy simulation using unstructured grids", in C. Liu and Z. Liu, editors, *Advances in DNS/LES*, Greyden Press, Columbus, Ohio, (1997) 117–128.

[4] K. E. Jansen, "Preliminary large-eddy simulations of flow around a NACA 4412 airfoil using unstructured grids", in *Annual Research Briefs*, Center for Turbulence Research, NASA Ames / Stanford University, (1995) 61–72.

[5] K. E. Jansen, "Large-eddy simulation of flow around a NACA 4412 airfoil using unstructured grids", in *Annual Research Briefs*, Center for Turbulence Research, NASA Ames / Stanford University, (1996) 225–232.

[6] T. J. R. Hughes, L. P. Franca, and M. Mallet, "A new finite element formulation for fluid dynamics: VI. Convergence analysis of the generalized SUPG formulation for linear time–dependent multidimensional advective–diffusive systems", *Comp. Meth. Appl. Mech. Engng.*, **63** (1987) 97–112.

[7] T. J. R. Hughes, L. P. Franca, and G. M. Hulbert, "A new finite element formulation for fluid dynamics: VIII. The Galerkin / least–squares method for advective–diffusive equations", *Comp. Meth. Appl. Mech. Engng.*, **73** (1989) 173–189.

[8] L. P. Franca and T. J. R. Hughes, "Convergence analyses of Galerkin / least–squares methods for symmetric advective-diffusive forms of the Stokes and incompressible Navier-Stokes equations", *Comp. Meth. Appl. Mech. Engng.*, **105** (1993) 285–298.

[9] P. Moin, K. Squires, W. H. Cabot, and S. Lee, "A dynamic subgrid–scale model for compressible turbulence and scalar transport", *Physics of Fluids*, **3** (1991) 2746–2757.

[10] P. Moin and J. Jimenéz, "Large–eddy simulation of complex turbulent flows", in *AIAA 24th Fluid Dynamics Conference.* AIAA-93-3099, (1993).

[11] M. Germano, U. Piomelli, P. Moin, and W. H. Cabot, "A dynamic subgrid–scale eddy viscosity model", *Physics of Fluids*, **3** (1991) 1760.

[12] G. Hauke, *A unified approach to compressible and incompressible flows and a new entropy-consistent formulation of thek-ϵ model*, Ph.D. thesis, Stanford University, 1995.

[13] F. Shakib, *Finite element analysis of the compressible Euler and Navier-Stokes equations*, Ph.D. thesis, Stanford University, 1989.

[14] L. P. Franca and S. Frey, "Stabilized finite element methods: II. The incompressible Navier-Stokes equations", *Comp. Meth. Appl. Mech. Engng.*, **99** (1992) 209–233.

[15] G. Hauke and T. J. R. Hughes, "A unified approach to compressible and incompressible flows", *Comp. Meth. Appl. Mech. Engng.*, **113** (1994) 389–396.

[16] K. E. Jansen and C. H. Whiting, "A generalized-α method for integrating the filtered Navier-Stokes equations with a stabilized finite element method", *Comp. Meth. Appl. Mech. Engng.*, (1999), Contributed to a special volume devoted to the Japan-US Symposium on F.E.M. in Large-Scale C.F.D.

[17] J. Chung and G. M. Hulbert, "A time integration algorithm for structural dynamics with improved numerical dissipation: The generalized-α method", *Journal of Applied Mechanics*, **60** (1993) 371–75.

[18] Z. Johan, T. J. R. Hughes, and F. Shakib, "A globally convergent matrix-free algorithm for implicit time marching schemes arising in finite element analysis", *Comp. Meth. Appl. Mech. Engng.*, **87** (1991) 281–304.

[19] F. Bastin, "Jet noise using large eddy simulation", in *Annual Research Briefs*, Center for Turbulence Research, NASA Ames / Stanford University, (1996) 115–132.

[20] J. Smagorinsky, "General circulation experiments with the primitive equations, I. The basic experiment", *Monthly Weather Review*, **91** (1963) 99–152.

[21] C. H. Whiting, K. E. Jansen, and S. Dey, "Hierarchical basis for stabilized finite element methods in fluid dynamics", *Comp. Meth. Appl. Mech. Engng.*, (1999).

[22] C. H. Whiting and K. E. Jansen, "A stabilized finite element method for the incompressible Navier-Stokes equations using a hierarchical basis", *International Journal of Numerical Methods in Fluids*, (1999).

[23] K. E. Jansen, S. S. Collis, C. H. Whiting, and F. Shakib, "A better consistency for low-order stabilized finite element methods", *Comp. Meth. Appl. Mech. Engng.*, **174** (1999) 153–170.

[24] T. J. R. Hughes, L. Mazzei, and K. E. Jansen, "Large-eddy simulation and the variational multiscale method", *Computing and Visualization in Science*, **to appear** (1999).

[25] K.E. Jansen, "Unstructured grid large eddy simulation of wall bounded flow", in *Annual Research Briefs*, Center for Turbulence Research, NASA Ames / Stanford University, (1993) 151–156.

[26] D. Carati, K. E. Jansen, and T. S. Lund, "A family of dynamic models for large-eddy simulation", in *Annual Research Briefs*, Center for Turbulence Research, NASA Ames / Stanford University, (1995) 35–40.

[27] D. Haworth and K. E. Jansen, "LES on unstructured deforming meshes: towards reciprocating IC engines", in *Proceedings of the 1996 Summer Program*, Center for Turbulence Research, NASA Ames / Stanford University, (1996) 329–346, also accepted for publication in Computers in Fluids.

[28] D. Coles and A. J. Wadcock, "A flying–hot–wire study of two–dimensional mean flow past an NACA 4412 airfoil at maximum lift", *AIAA Journal*, **17** (1979) 321.

[29] R. C. Hastings and B. R. Williams, "Studies of the flow field near a NACA 4412 aerofoil at nearly maximum lift", *Aero J.*, **91** (1987) 29.

[30] A. J. Wadcock, "Investigation of low–speed turbulent separated flow around airfoils", Technical Report 177450, NACA CR, 1987.

[31] J.W. Deardorff, "A numerical study of three-dimensional turbulent channel flow at large Reynolds numbers", *Journal of Fluid Mechanics*, **41** (1970) 453.

[32] P.R. Spalart, W.H. Jou, M. Stretlets, and S.R. Allmaras, "Comments on the feasibility of LES for wings and on a hybrid RANS/LES approach", in *Advances in DNS/LES*, Greyden Press, Columbus, (1997) 137–147.